LAWRENCE
LIVERMORE
NATIONAL
LABORATORY

UCRL-TR-207056

KCAT, Xradia, ALS and APS Performance Summary

A. Waters, H. Martz, W. Brown

October 5, 2004

This work was performed under the auspices of the U.S. Department of Energy by University of California, Lawrence Livermore National Laboratory under Contract W-7405-Eng-48.

KCAT, Xradia, ALS and APS Performance Summary[1]

Amy Waters, Harry Martz, and William Brown
UCRL-TR-207056
Lawrence Livermore National Laboratory

Introduction

At Lawrence Livermore National Laboratory (LLNL) particular emphasis is being placed on the nondestructive characterization (NDC) of components, subassemblies and assemblies of millimeter-size extent with micrometer-size features (mesoscale). These mesoscale objects include materials that vary widely in composition, density, geometry and embedded features. Characterizing these mesoscale objects is critical for corroborating the physics codes that underlie LLNL's Stockpile Stewardship mission. In this report we present results from our efforts to quantitatively characterize the performance of several x-ray systems in an effort to benchmark existing systems and to determine which systems may have the best potential for our mesoscale imaging needs.

Several different x-ray digital radiography (DR) and computed tomography (CT) systems exist that may be applicable to our mesoscale object characterization requirements, including microfocus and synchrotron systems. The systems we have benchmarked include KCAT (LLNL developed) and Xradia μXCT (Xradia, Inc., Concord, CA), both microfocus systems, and Beamline 1-ID at the Advance Photon Source (APS) and the Tomography Beamline at the Advanced Light Source (ALS), both synchrotron based systems. The ALS Tomography Beamline is a new installation, and the data presented and analyzed here is some of the first to be acquired at the facility. It is important to note that the ALS system had not yet been optimized at the time we acquired data. Results for each of these systems has been independently documented elsewhere [*Waters, et al. 2004; Waters et al. 2004a; Brown, et al. 2004; Gross, et al. 2004]*. In this report we summarize and compare the characterization results for these systems.

Reference standards and DR/CT MTF objects

In FY03, two reference standards were fabricated and characterized using metrology tools. One of the reference standards was built with a cylindrical geometry and contained features similar to those on a Super Nova Raleigh Taylor (SNRT) target, and the other reference standard was built with a spherical geometry and contained features similar to those on a double shell target. The standards were designed for manufacturability, stability and to provide a range of features that can be measured using NDC methods. For reference standard fabrication details and metrology results, see Hibbard, et al. 2004.

In FY04 we developed several NDC tools and procedures that were used to quantitatively characterize the performance of the systems above. In addition to the two mesoscale reference

[1] *This work was performed under the auspices of the U.S. Department of Energy by University of California, Lawrence Livermore National Laboratory under Contract W-7405-Eng-48.*

standards, additional test objects were used in an effort to characterize the performance of the x-ray systems. A thin (0.51 mm) polished tantalum (Ta) edge, as well as eight gold-coated copper (Au-Cu) edges were used to determine DR modulation transfer functions (MTF) and a set of three commercially made hollow tubes were used to determine CT MTFs for each system. In addition to the Au-Cu edges, a new set of six tungsten edges was fabricated for future use with higher energy x-ray systems (up to 200 kV). These edges are described in greater detail by Logan, et al. 2004.

To determine the DR MTF for an x-ray system, a transmission image of the edge was acquired, and a 10-pixel wide one-dimensional lineout measured across the edge. The derivative of the lineout was determined, resulting in the edge-spread function. The Fourier transform of this edge-spread function is the line-spread MTF [*Hasegawa, 1991; Logan, et al. 1998*]. The MTF is a frequency-domain description of the spatial resolution of an imaging system or component, and thus the MTF of a system is the product of the MTFs of each of the various system components. The DR MTF for each system was measured using the Ta edge and several systems were quantified using the Au-Cu edges. We have shown that the MTFs measured using the Ta and Au-Cu edges correlate very well and that comparisons can be made directly between the edges across systems. [*Waters, et al. To be published*] The variance for one Au-Cu edge between multiple MTF measurements at 20 lp/mm is less than 4%, and increases with spatial resolution.

The CT MTF was also measured for KCAT using inexpensive commercial tubing. We used three tubes that differ in composition (low-density polyethylene [LDPE], copper and gold), outer diameter, and wall thickness in an effort to best represent double-shell capsules of LLNL programmatic interest [*Logan, et al. 2004*]. Tubes were selected instead of solid objects because all HEDP capsule designs have a “cavity”, and imaging of inside surfaces is a far greater challenge to a CT system than imaging the outside edge of an object. From CT reconstructions of the tubes, we measured the MTF of both the inner and outer edges by taking a lineout, calculating the derivative and performing a Fourier transform, as described above.

None of the MTF results presented here have been clipped or smoothed in any way. While this results in MTF curves that appear noisier than some, they are a true representation of the system, and any and all noise present is a direct result of the system components.

System performance measurements

A summary of the system parameters used to acquire DR images for the Ta and Au-Cu edges is presented in Table 1. The DR MTFs measured with the Ta edge for each of the four x-ray systems is presented in Figure 1.

Table 1. Summary of system parameters used to acquire DR data.

	KCAT	Xradia μXCT	ALS	APS 1-ID
energy	60 kV	60 kV	6 keV	10 keV
current	0.08	0.1	-	-
source-to-object distance (mm)	54	~90	-	-
object-to-detector distance (mm)	106	~10	~100	262
Scintillator	Terbium-doped glass	CsI	Cd_2WO_4	Cd_2WO_4
Scintillator to CCD coupling	NIKON 60 mm Micro-Nikkor lens	Microscope objective and tube lens	LLNL designed Hoya manufactured lens	Mitutoyo 10X microscope lens
Camera	Apogee	Andor	Quantix	Princeton Instruments
Camera bits	14	16	12	12
Camera pitch (μm)	9	13	9	25
Pixel size at object (μm)	3	2.3, 0.5*	3.3	2
DR I acquisition time (sec)	300	60	4.5	0.5
No. of frames averaged	2	1	1	1 or 2
DR I_0 acquisition	300	300	4.5	N/A
No. or frames averaged	2	4	1	N/A
Total Time (sec)	1200	1260	9	<60

*Note: Xradia μXCT system has two modes: high and low resolution. The 1:1 (without geometric magnification) pixel size in high resolution mode is 0.5 μm, and in low resolution mode it is 2.7 μm.

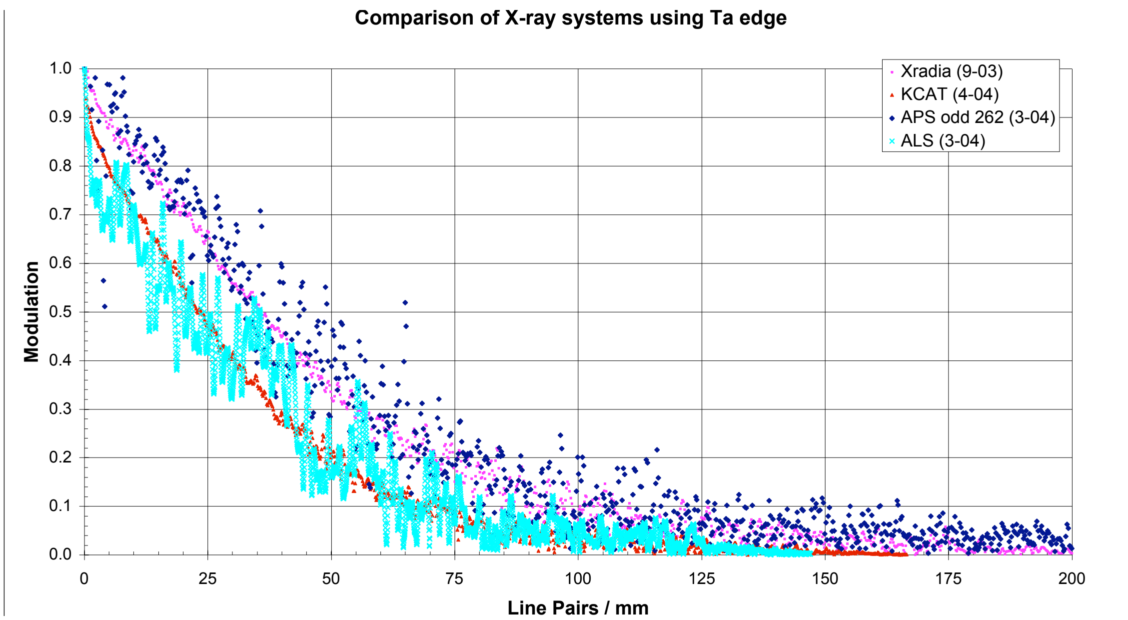

Figure 1. DR MTFs measured with the Ta edge for four x-ray systems. Xradia data is presented for the low resolution mode. Note that the APS and ALS curves both appear very noisy compared to the Xradia and KCAT data. Also, note that the MTF values for the Xradia and the APS data appear higher than the KCAT and ALS data.

The DR MTF was also measured for Xradia in the high-resolution mode (pixel size at object ~0.5 μm). Results for the Ta and Au-Cu edge are presented in Figure 2, as well as a comparison of MTF curves for high- and low-resolution modes.

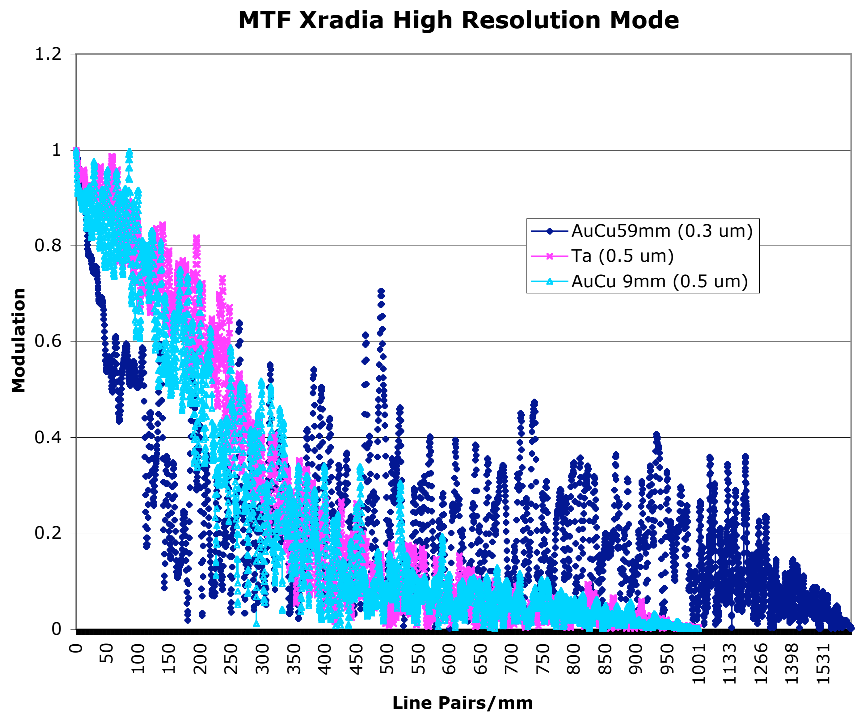

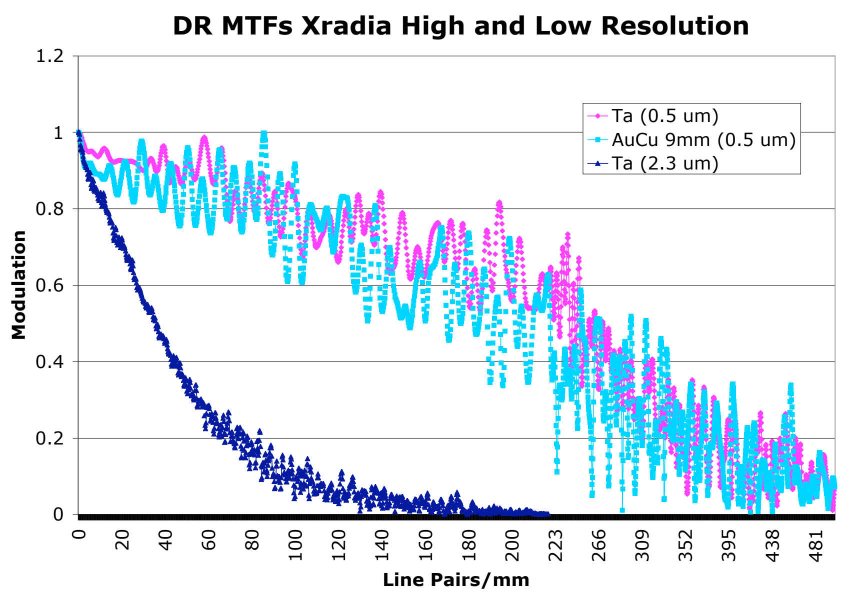

Figure 2. Top: DR MTF measurements for Xradia μXCT system in high-resolution mode. Measurements were made with the Ta edge at 9 mm from the detector and one Au-Cu edge at 59 mm and 9 mm from the detector. Bottom: comparison of MTF measurements for Xradia high- and low-resolution mode.

Signal-to-noise ratios (SNRs) were also measured for each system using the transmission images of the Ta edge. The SNR is defined as the difference between the mean of two signals (in our case the two signals are within, S_1, and outside, S_2, the Ta edge) divided by the square root of the sum of the squares of the standard deviation, σ:

$$\frac{S_1 - S_2}{\sqrt{\sigma_1^2 + \sigma_2^2}},$$

where S is the mean of the signal. Three SNR measurements were made for each system and are presented in Table 2.

Table 2. Two-dimensional SNRs measured for each system.

System	Size of area (pixels)	SNR	Average SNR
KCAT	153 x 151	149.4	
	148 x 150	146.8	
	148 x 151	96.6	130.9 ± 29.8
Xradia low resolution	158 x 159	128.5	
	154 x 153	93.4	
	158 x 152	126.6	116.2 ± 19.7
Xradia lhigh resolution	149 x 144	68.4	
	154 x 156	64.0	
	149 x 153	58.8	63.7 ± 4.8
ALS	150 x 150	47.1	
	150 x 150	41.2	
	150 x 150	46.0	44.7 ± 3.2
APS	147 x 149	15.7	
	148 x 151	21.7	
	147 x 151	11.0	16.1 ± 5.4

Transmission (I/I_0) images of the spherical reference standard were acquired with each of the four x-ray systems and are shown in Figure 3.

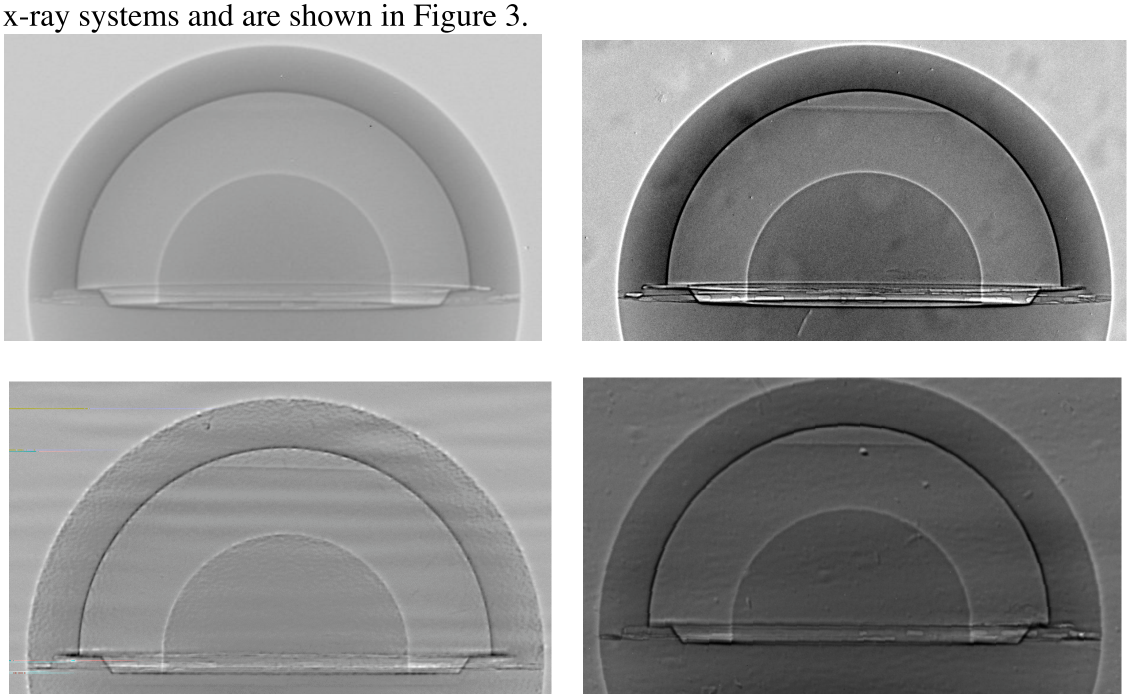

Figure 3. Transmission images of the spherical mesoscale reference standard acquired with four x-ray systems. Top left: KCAT, Top right: Xradia, Bottom left: ALS, Bottom right: Beamline 1-ID APS.

CT MTF measurements were made for only the KCAT system using the LDPE, Cu and Au tubes. Scan parameters used to acquire CT data for the tubes are presented in Table 3 and a CT slice from each tube is shown in Figure 4. Computed tomography MTF results for the inner and outer diameters of each tube are presented in Figure 5.

Table 3. KCAT scan parameters used to acquire CT data for the tubes.

Material	Energy (kV)	Current (mA)	s.o.d.* (mm)	o.d.d.+ (mm)	Integration time (s)	No. frames averaged	No. projections
LDPE	60	0.08	50	100	160	4	360
Cu	140	0.03	50	100	100	4	450
Au	140	0.03	50	100	100	4	450

*source-to-object distance; +object-to-detector distance

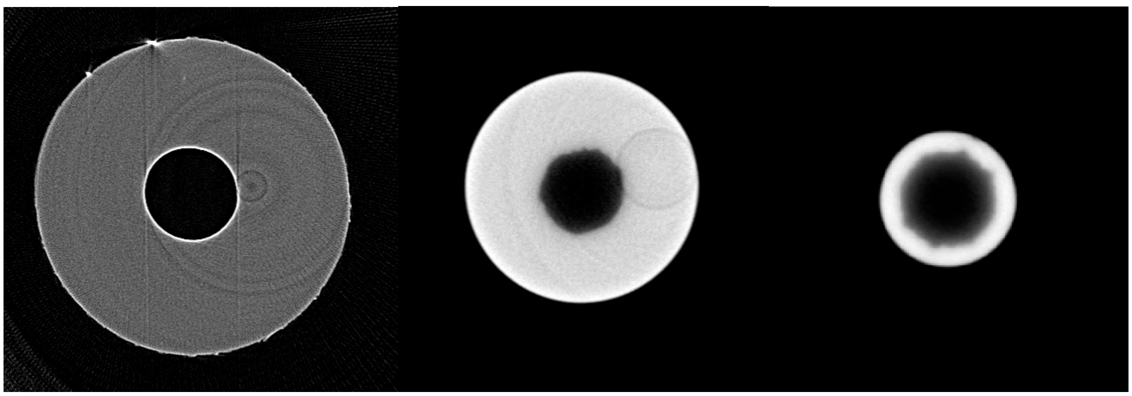

Figure 4. CT slices from LDPE (left), Cu (middle) and Au (right) tubes.

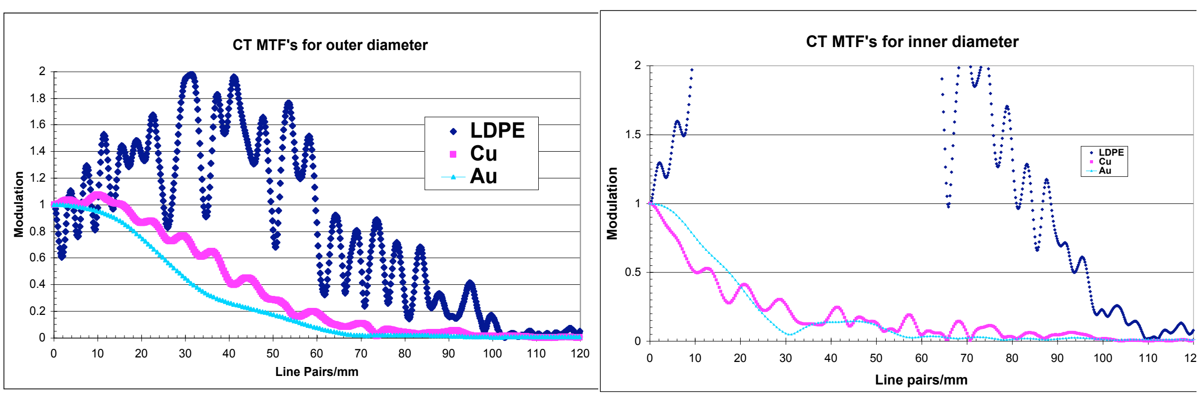

Figure 5. MTF measurements determined from CT images of LDPE, Cu and Au tubes. MTFs were measured for the inner (right) and outer (left) edges of the tubes from one 10-pixel wide radial lineout. Note the anomalous LDPE MTF result. This most likely is due to the strong phase effects observed in the data.

Computed tomography data was acquired for the spherical reference standard using KCAT, Xradia and ALS. The APS images could not be reconstructed into CT slices because the beamline was not set up to acquire CT data. While a series of projections was acquired, it required translating the reference standard between rotation, resulting in a data set with serious registration problems. A summary of CT scan parameters used to acquire data is presented in Table 4. Representative CT slices of the spherical reference standard acquired with each of the systems is presented in Figure 6.

Table 4. A summary of CT scan parameters used to acquire data for the spherical reference standard.

System	No. Projections	Angular range (deg)	Pixel size at object (μm)	Time per projection (sec)	No. frames averaged	Energy	Current (mA)	Total time (hrs)
KCAT	360	360	3	300	2	60 kV	0.08	60
Xradia	721	180	1.45	80	1	60 kV	0.1	16
ALS	360	180	3.34	4.5	1	6 keV	-	0.5

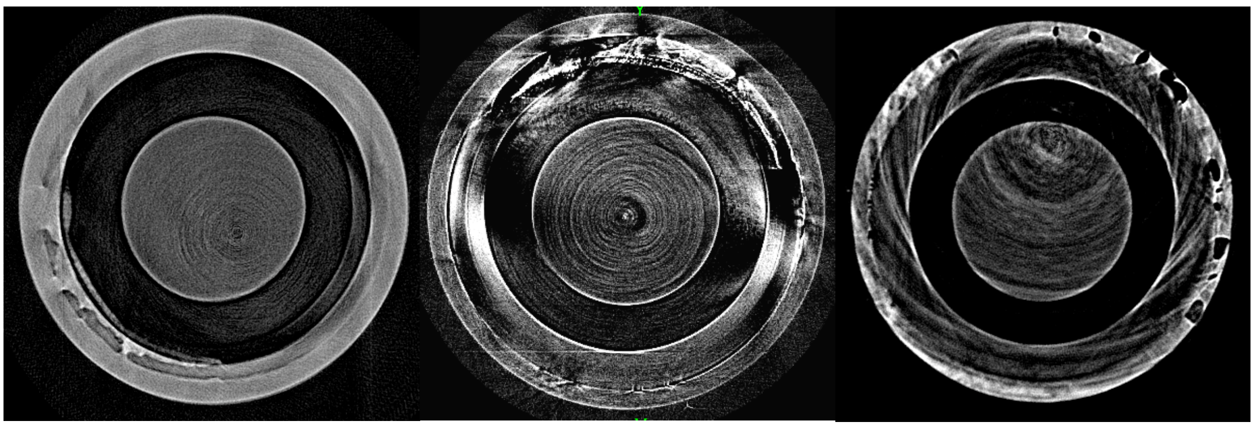

Figure 6. CT slices from the spherical reference standard acquired with KCAT (left), Xradia μXCT (middle) and ALS (right). The slices are not taken from the same location in the reference standard.

Results and Discussion

DR system performance

A comparison of the MTFs for the four systems, shown in Figure 1, reveals some interesting performance results. It appears that the two synchrotron based systems (APS and ALS) have much noisier MTF curves than the two microfocus systems (KCAT and Xradia). APS yielded the highest MTF curve of any of the systems, while ALS and KCAT yielded the lowest. It is also interesting to note that Xradia and APS have similar MTF curves, and KCAT and ALS also have similar MTF curves.

The Xradia high-resolution mode gives MTF values that are much higher than the low-resolution mode (Figures 2 and 3). Comparing the Ta edge MTF curves at high- and low-resolution (Figure 3), at 50 lp/mm (correlating to a spatial resolution of 10 μm), the Ta edge MTF in low-resolution mode has a value of 0.32, while in high-resolution mode, the Ta edge MTF is 0.93. This is difference of 65%. However, the MTF curve in the high-resolution mode is much noisier than the low-resolution mode. The goal of our mesoscale imaging effort is to achieve a spatial resolution of less than 1 μm, which correlates to 500 lp/mm in the frequency domain. At 500 lp/mm the Xradia μXCT system in high-resolution mode yields MTF values near 0.1, or 10%.

A comparison of SNR measurements (Table 2) reveals that KCAT has the highest average SNR, followed by Xradia, and then ALS. APS had the lowest average SNR of all the systems. That the synchrotron systems have the lowest SNR measurements is not unexpected, given their noisy

MTF curves. We can conclude that while the synchrotron systems are significantly faster in terms of data acquisition, the resulting data is much noisier than the lab based microfocus systems, which is somewhat surprising.

X-ray system component comparisons

For the following discussion, please refer to Table 1. The x-ray energy used in the data acquisition is the same for the microfocus systems (60 kV), and is similar for the synchrotron systems (6 and 10 keV). Also, the flux for the microfocus systems is nearly the same (0.08 and 0.1), and similar for the synchrotron systems. KCAT was the only system to use significant geometric magnification (3X), however resulting effective pixel size at the object was similar across each of the systems (2 to 3.3 μm), excluding the Xradia high-resolution mode (0.5 μm). Thus, we can conclude that the differences in MTF observed in Figure 1 are not due to the scan parameter settings mentioned above, and we must look elsewhere for the cause of the differences.

The detector systems are the biggest difference between the x-ray systems. The KCAT system uses a thick terbium-doped scintillating glass with a camera lens coupled to a 14-bit CCD camera to acquire images. The Xradia system uses a thin CsI scintillator with both a microscope objective and a tube lens coupled to a 16-bit CCD camera to acquire data. Both synchrotron systems employ a Cd_2WO_4 scintillator coupled to a 12-bit CCD camera, but the APS scintillator is thinner than that used by ALS. ALS uses a camera lens to couple to the CCD camera for data acquisition, while APS uses a 10X objective lens. Note that the camera pixel pitch on the KCAT and ALS systems is smallest, 9 μm, compared to the APS and Xradia systems, with 25 μm and 13 μm, respectively. It appears that the superior MTF curves for the APS and Xradia systems, despite their larger camera pixel pitch. may be due to their use of a microscope lens coupled with a thin scintillator.

The time required to acquire DR images (and, consequently, CT data) ranges from seconds (synchrotron systems) to tens of minutes (microfocus systems). APS provides the fastest data acquisition, with ALS close behind. The slowest system is Xradia, with a total acquisition time of 1260 seconds. KCAT is second slowest with 1200 seconds. Time does not appear to correlate with superior MTF values. While ALS and APS provide the fastest DR data acquisition times, it is usually not easy or convenient to get beam time at synchrotron facilities. The lab-based Xradia system provides spatial resolution equivalent to the APS. Thus, if time is not an issue, one can get spatial resolutions equivalent to synchrotron systems using more convenient and much smaller lab systems.

KCAT CT system performance

We have begun to develop the methodology to measure MTF curves for CT data using the three tubes. KCAT was the only system available for this analysis at the time of this report, but it would be very useful to performance identical analyses on the other three systems. Analysis of the CT data shown in Figure 4 reveals bright edges surrounding the LDPE inner and outer edges. These bright edges are due to phase effects. The Cu and Au tubes do not show phase effects but do show significant non-uniformities near the inner diameters. The inner diameters of the Cu and Au tubes do not appear round, and have notches. The LDPE CT MTF data acquired with KCAT (Figure 5) appears significantly different for both inner and outer edges when compared to the Cu and Au data. This is most likely due to phase effects [*Schneberk, et al. 2004*]. The LDPE CT MTF curve is not useful as an indicator of system performance because it is not physically possible to have MTF values greater than one (MTF can never exceed a sinc function [sin(x)/x], where x is the pixel size at the object). The MTF measurements for the Au and Cu tubes appear reasonable, as expected due to the lack of apparent phase effects in the CT slices. It is not unexpected that the inner diameter MTF measurements are significantly lower than the outer diameter MTF measurements. In fact, one would expect the CT MTF of the outer diameter to approach the DR MTF while scatter from the object dramatically decreases the MTF measurements on the inner diameter. At 20 lp/mm, the outer diameter MTF for the Cu and Au tubes is ~0.9 and ~0.75, respectively, while the inner diameter MTF values are around 0.4 for both tubes. This is a decrease of more than 55% for Cu and more than 65% for Au from outer to inner edge. Although the decrease in MTF from outer to inner edge is expected, the actual values of more than 50% are more significant than expected.

Characterization of spherical reference standard

The DR transmission images of the spherical reference standard shown in Figure 3 do not appear dramatically different. This is expected, given the similar MTF curves for each system. Note that the top edge of the aerogel can be seen in each image, and the step joint appears to be non-uniform. Each of the images shows phase effects as expected, as evidenced by the bright and dark regions surrounding all of the edges.

The CT slices of the spherical reference standard shown in Figure 5 all show similar features in the object. The area near the step joint shows many unbonded regions in each image, as well as some excess material, probably glue. The Xradia and ALS data show more artifacts such as streaking, and ring artifacts, than the KCAT data. The time required to acquire the KCAT data (60 hours) was more than a factor of 100 greater than the time required to acquire the ALS data (0.5 hours). The Xradia data acquisition time was 16 hours.

Summary

We have developed test objects and reference standards to assist in our efforts to quantify x-ray system performance for mesoscale imaging applications. We used these objects and reference standards to benchmark the system performance of four x-ray DR/CT systems: KCAT, Xradia, APS and ALS. We found that the systems yielding the highest MTF curves, Xradia and APS, both used detector systems comprised of a thin scintillator coupled by a microscope lens to a CCD camera. We also found that the synchrotron systems (APS, ALS) yielded much noisier curves than those from the microfocus systems (KCAT, Xradia), yet acquired data much faster. The microfocus systems provided the highest signal to noise ratios, compared to the synchrotron systems. The CT MTF results showed that MTF decreases significantly from outer to inner edges of an object, as expected. In addition, we acquired DR and CT data for the reference standards to begin characterization of the as-built objects.

Future work includes measuring CT MTF curves for all four systems, as well as understanding more fully the effects of phase on all the data. A more detailed system error analysis would also be useful as an additional benchmark of system performance. Finally, the three-dimensional data acquired with the x-ray systems should be analyzed in a way to extract quantitative dimensional information about complex mesoscale objects. Information that should be extracted includes void content, bond/joint integrity, sphericity/concentricity of components, and overall as-built quality.

References

Brown, W., A. Waters, and H. Martz, "ALS Performance Summary – Update", Lawrence Livermore National Laboratory, CA, UCRL-TR-207808 (2004).

Gross, J., B. Kozioziemski, A. Waters and H. Martz, "APS Performance Summary – Update", Lawrence Livermore National Laboratory, Livermore, CA, UCRL-TR-207260 (2004).

Hasegawa, B., *The Physics of Medical Imaging*, Madison, WI, Medical Physics Publishing (1991).

Hibbard, R., M. Bono, A. Waters and H. Martz, "FY03 Technology Base Final Report for: Production and Documentation of Meso-Scale Metrology and Characterization Reference Standards, Cylindrical and Spherical", Lawrence Livermore National Laboratory, Livermore, CA, *To be published* (2004).

Logan, C., J. Haskins, K. Morales, E. Updike, J. Fugina, T. Lavietes, D. Schneberk, G. Schmid, K. Springer, P. Soltani, and K. Swartz, "Evaluation of an Amorphous Selenium Array for Industrial X-ray Imaging", Lawrence Livermore National Laboratory, Livermore, CA, UCRL-ID-132315 (1998).

Logan, C., A. Waters and H. Martz, "Edges for Digital Radiography and NIF HEDP Capsule Phantoms for Computed Tomography," Lawrence Livermore National Laboratory, Livermore, CA, UCRL-ABS-207064 (2004).

Schneberk, D. J., H. E. Martz, and W. D. Brown, "Dimensional Measurements of Three Tubes by Computed Tomography", Lawrence Livermore National Laboratory, Livermore, CA, UCRL-TR-207195 (2004).

Waters, A., H. Martz, C. Logan, J. Gross and D. Chinn, "KCAT Performance Summary – Update, Revision 1", Lawrence Livermore National Laboratory, Livermore, CA, UCRL-TR-203519-REV-1 (2004).

Waters, A., H. Martz, C. Logan, J. Gross and D. Chinn, "Xradia Performance Summary – Update", Lawrence Livermore National Laboratory, Livermore, CA, UCRL-TR-206565 (2004a).

Waters, A., D. Schneberk, W. Brown and H. Martz, "DR and CT MTF Measurements for Mesoscale Imaging Systems", Lawrence Livermore National Laboratory, Livermore, CA, *To be published.*